Validation of Satellite Soil Moisture Products by Sparsification of Ground Observations

Longfei Hao, Jingjing Chen, Zushuai Wei, Linguang Miao, Tianjie Zhao, *Senior Member, IEEE*, and Jian Peng

***Abstract*—Dense soil moisture observation networks serve as the primary means to validate large-scale satellite soil moisture products. However, maintaining intensive observation demands substantial labor and financial resources. It is therefore crucial to address the issue of how to sparsify ground observations while still achieving comparable validation results. Accordingly, this study takes an agropastoral interconnected zone of the Shandian River basin as an example. Representative soil moisture sites and the minimal number of required sites (NRS) were investigated at different sampling depths (3 and 50 cm) and at multiple scales (3, 9, 36, and 100 km). The average soil moisture estimated from the representative sites was then applied to validate SMAP L2, L3, and L4 multiscale soil moisture products. The findings indicate that the spatial heterogeneity of soil moisture within the Shandian River basin remained relatively consistent across varying spatial scales. However, it exhibited a notable increase in heterogeneity when moving vertically into deeper soil layers. Representative sites can more accurately determine the average soil moisture in a region, showing that SMAP notably overestimated root zone soil moisture and underestimated surface soil moisture. This research can serve as a theoretical guide for watershed-scale soil moisture estimation as well as a solid scientific foundation for improving the architecture of the watershed soil moisture network.**

***Index Terms*—Representativeness, SMAP, Shandian River basin soil moisture network (SMN-SDR), soil moisture, temporal stability analysis, validation.**

I. Introduction

SOIL moisture plays a crucial role in regulating water, energy, and carbon exchange processes between the surface and atmosphere, making it a vital component of the global water cycle system [1], [2], [3]. Accurate soil moisture information is therefore an essential input parameter for hydrological, climate, land surface, and ecological models [4], [5], [6]. In the context of global climate change, soil moisture observations are particularly important, as anomalous climate changes can substantially impact the global water cycle, leading to extreme hydrological events such as floods and droughts [7], [8], [9]. Therefore, obtaining highly accurate soil moisture products is critical for facilitating hydrological and ecological-related applications.

Large-scale soil moisture monitoring has been made possible by the development of remote sensing technology, which links changes in soil moisture using the soil surface's spectral reflectance properties, the intensity of electromagnetic radiation, or the backscattering coefficient [10]. Various remote sensing techniques have been employed to monitor soil moisture in accordance with the physical characteristics of soil and related radiation theory because soil moisture exhibits varied characteristic responses in different electromagnetic wavelength bands. Due to its solid physical foundation, microwave soil moisture remote sensing is especially advantageous, capitalizing on the difference in dielectric properties between dry soil and liquid moisture to estimate soil moisture. Moreover, microwave remote sensing is a valuable tool for soil moisture estimation due to its all-weather capability and ability to penetrate through vegetation [11]. As a result, microwave remote sensing has become a primary data source for soil moisture observations [12]. The use of passive microwave sensors as satellite payloads has led to the development of various retrieval algorithms for different soil moisture products [13]. However, there are still uncertainties in the accuracy of these satellite-based soil moisture retrievals, highlighting the need for validation through *in situ* data.

Validating passive microwave soil moisture products using ground measurements has been challenging due to differences in spatial scale and representativeness between site observations and remote sensing data, as pointed out by studies such as Crow et al. [14] and Whitcomb et al. [15]. Effective upscaling algorithms can derive average soil moisture conditions on a large scale from limited ground observations [16]. Common upscaling methods for estimating areal average soil moisture from limited ground observations include temporal stability [17], geostatistical methods [18], land surface models [19], and methods based on remote sensing observations [20], etc. To improve the efficiency and robustness of validation, it is often helpful to combine different upscaling methods and choose

Manuscript received 20 September 2023; revised 13 November 2023, 15 January 2024, and 25 January 2024; accepted 1 February 2024. Date of publication 6 February 2024; date of current version 12 March 2024. This work was supported in part by the National Natural Science Foundation of China under Grant 42301441 and in part by the Research Fund of Jianghan University under Grant 2023JCYJ13. *(Corresponding author: Zushuai Wei.)*

Longfei Hao and Linguang Miao are with the School of Surveying and Land Information Engineering, Henan Polytechnic University, Jiaozuo 454150, China (e-mail: haolongfei@home.hpu.edu.cn; miaolinguang@home.hpu.edu.cn).

Jingjing Chen is with the School of Architecture Engineering, Xinyang Vocational and Technical College, Xinyang 464000, China (e-mail: chen jingjingw99@163.com).

Zushuai Wei is with the School of Artificial Intelligence, Jianghan University, Wuhan 430056, China (e-mail: weizushuai@whu.edu.cn).

Tianjie Zhao is with the State Key Laboratory of Remote Sensing Science, Aerospace Information Research Institute, Chinese Academy of Sciences, Beijing 100101, China (e-mail: zhaotj@aircas.ac.cn).

Jian Peng is with the Department of Remote Sensing, Helmholtz Centre for Environmental Research–UFZ, 04318 Leipzig, Germany, and also with the Remote Sensing Centre for Earth System Research, Leipzig University, 04103 Leipzig, Germany (e-mail: jian.peng@ufz.de).

Digital Object Identifier 10.1109/JSTARS.2024.3362833

optimal site locations. Among them, identifying representative stations through temporal stability analysis has been proven effective for predicting the areal average soil moisture condition. With the emergence of China's new mission, the Terrestrial Water Resources Satellite, the comprehensive validation of this satellite on a national or even global scale will require a large number of ground observations for support [35]. Since network layout and maintenance are resource-intensive, and dense ground observation sites are not always available, identifying representative sites for estimating the areal average soil moisture can save considerable human and material resources [7], [21].

Temporal stability is defined as a time-invariant correlation between spatial locations and classical statistical parameter values [22]. This concept suggests that specific locations within an area maintain their stability over time, which can be leveraged to reduce the number of required sampling points while enhancing sampling efficiency and maintaining accuracy standards [23]. Previous studies have demonstrated the effectiveness of temporal stability analysis and have introduced this concept to the study of soil moisture observations [24], [25], [26], [27], [28], [29], serving as a valuable tool for validating satellite soil moisture products [7], [17], [30], [31], [32]. Starks et al. [28] demonstrated that temporal stability analysis is an efficient method for validating satellite soil moisture products using the Little Washita River Soil Moisture Network in Oklahoma. Chen et al. [7] performed temporal stability analysis over a 5000 km^2 area based on the Maqu soil moisture network, selected representative stations at multiple depths, and used representative stations to estimate areal average soil moisture when data were missing. Yee et al. [32] employed temporal stability analysis and geostatistical analysis to identify multiscale representative stations using long-term soil moisture observations from the Yanco area, which were effectively applied in the subsequent validation of AMSR2 and SMOS [21]. The concept of temporal stability has also been utilized in some studies to analyze the spatial distribution of satellite soil moisture products and select representative pixels [33], [34], thereby optimizing the process of satellite validation.

In previous satellite soil moisture product validation studies, *in situ* soil moisture data were predominantly obtained from regions with high-density networks in Europe and the United States. To fill the gap, the Shandian River basin Soil Moisture Network (SMN-SDR) was established to provide long-term *in situ* soil moisture data for validating soil moisture products in China [35]. Although previous studies have comprehensively validated major remotely sensed soil moisture products using SMN-SDR [2], [12], there has been no investigation into the representativeness of sites in the region. Therefore, it is necessary to determine the spatial representativeness of different sites in the area to reduce the uncertainty of the validation results. The long time series soil moisture data accumulated by SMN-SDR can be used to match soil moisture products at different scales and depths [35], providing a valuable opportunity for conducting multiscale and multidepth temporal stability analysis and soil moisture product validation.

Based on SMN-SDR soil moisture data and manual ground sampling data, this study investigated the spatial and temporal variation characteristics of soil moisture in the area. Accordingly, the representativeness of each site at multiple scales and depths was evaluated by using temporal stability analysis. The minimal number of required sites (NRS), which can be used to estimate the regional soil moisture in the Shandian River basin, was determined. Lastly, the identified representative sites were used to validate the SMAP L2, L3, and L4 soil moisture products and analyze the impact of the number of sites on the validation results.

II. Study Area and Datasets

A. Overview of Shandian River

The study area is situated in the upper reaches of the Luan River, within the Shandian River basin, spanning across the Hebei and Inner Mongolia autonomous regions of China. The region has a temperate continental climate with an average annual temperature ranging from 5 to 7 °C. The area experiences an average annual rainfall between 300 and 500 mm, which primarily occurs during the months of July to September. Winters are cold and dry, and the area is characterized by seasonal frozen soil. The topography of the region is relatively flat and comprises mainly plains and hills, while the land cover includes grasslands, farmlands, and forests [2], [12], [35].

B. Shandian River Network

The Shandian River basin is equipped with a nested automatic soil temperature, moisture, and precipitation network that operates at multiple scales and layers. The network covers an area of 1° × 1° (115.5 °E–116.5 °E, 41.5 °N–42.5 °N) and includes 34 stations installed at spatial resolutions of 100, 50, and 10 km. The purpose of the network is to validate satellite- and model-based soil moisture products at various spatial resolutions. To measure soil moisture and temperature, Decagon 5TM sensors were installed at each station. These sensors operate at five depths, which are 3, 5, 10, 20, and 50 cm. Data were recorded every 10 min before June 2019 and every 15 min thereafter [35].

This study used soil moisture and temperature data collected at depths of 3 and 50 cm from September 16, 2018 to December 31, 2019, with the data publicly available from the International Soil Moisture Network (ISMN) website.[1] To match SMAP soil moisture products with different spatial resolutions, sites in the study area were reprojected onto the EASE-2 grids at scales of 3, 9, and 36 km (as shown in Fig. 1). Specifically, eight sites (S1–S8) were located within SMAP 9 km pixels as core validation sites, 14 sites (S1–S8, M2, M6, M7, M8, M9, and M11) were situated within SMAP 36 km pixels, and other sites were evenly distributed across various locations in the area. The daily mean values of soil moisture were used to analyze temporal stability.

C. Field Sampling Campaign

To provide accurate reference data for remote sensing observations, a field sampling campaign was conducted from September 16 to September 26, 2018, in conjunction with an airborne

[1] [Online]. Available: https://ismn.earth/en/

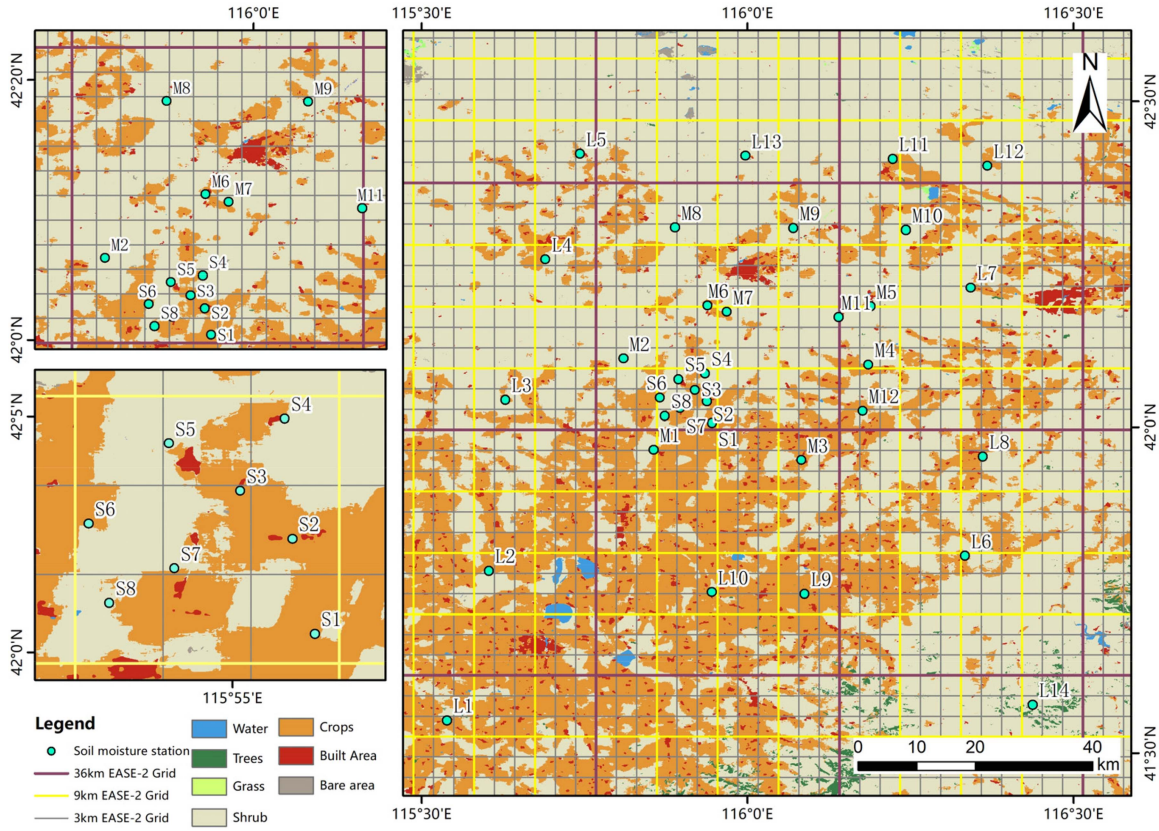

Fig. 1. Land use in the Shandian River basin and layout of 34 sites in the SMN-SDR. Left insets show the distribution of sites within the 9 and 36 km EASE-2 grids (top: 36 km, bottom: 9 km).

campaign. The manual ground sampling data were collected by setting up 30 sample areas within a 70 km × 12 km experimental region, with each area measuring 1 km × 2 km and containing 4–6 sample plots. Sampling points were placed in the middle of each sample plot at intervals of 50–100 m, and the 0–5 cm soil moisture volumetric content was measured using a Delta-TML3 soil moisture meter. Each sample point was measured 3–6 times, and the mean value was taken as the true value for that point. Soil samples were also collected from each sample area, and the Delta-TML3 sensor soil moisture data was calibrated using the oven-drying method in the laboratory [35]. Finally, the study utilized manual ground sampling data within the 9 km pixel of SMAP, with data from other sampling points excluded.

D. SMAP Soil Moisture Products

The Soil Moisture Active Passive (SMAP) satellite, launched by NASA in January 2015, was designed primarily for observing global soil moisture. It operates on a Sun-synchronous orbit at an altitude of 685 km and is equipped with an *L*-band radar (1.22–1.3 GHz) and an *L*-band radiometer (1.4 GHz). However, the radar stopped functioning on July 7, 2015. With a temporal resolution of 1–3 days, SMAP can cover 95% of the global land area every day and provide data updates every 2–3 days [36]. The overpass time of SMAP is 6:00 A.M. and 6:00 P.M. solar synchronous time, and the surface soil moisture is estimated with a target accuracy of 0.04 m^3/m^3. The L2, L3, and L4 soil moisture data of SMAP are all projected to EASE-2 grids [37].

This study utilized various SMAP soil moisture products ranging from September 16, 2018, to December 31, 2019. The L2 soil moisture products include the SPL2SMAP_S, which has a 3 km spatial resolution, and is synthesized using SMAP *L*-band brightness temperature and Sentinel-1 *C*-band backscattering coefficient [38], [39]. The L3 soil moisture products include the daily composite SPL3SMP_E (has a grid size of 9 km) and SPL3SMP (36 km spatial resolution) soil moisture products derived from L2 soil moisture data [37], [40]. This study only used the L2 and L3 descending orbit data. In addition, the L4 soil moisture product, SPL4SMGP, which has a nominal spatial resolution of 9 km, was obtained by assimilating SMAP brightness temperature data into the catchment land surface model [2], [41].

III. Methods

A. Spatiotemporal Variability of Soil Moisture

The spatiotemporal variability of soil moisture is crucial for modeling land surface processes and scaling conversions. Famiglietti et al. [42] and Zhao et al. [35] have emphasized the importance of understanding the spatiotemporal characteristics of soil moisture, especially in the Shandian River basin, to improve the use of remotely sensed soil moisture products. Although Zhao et al. [35] studied the coefficient of variation

using manual ground sampling data, they found that the spatial variability in the region is complex and affected by multiple factors, which require further investigation. Therefore, this article employs SMN-SDR soil moisture data to investigate the temporal changes in the mean, standard deviation, and coefficient of variation of soil moisture. In addition, it analyzes the spatial heterogeneity of soil moisture at different depths and scales.

The formulas for the spatial average value (Avg), standard deviation (Std), and coefficient of variation (CV) of soil moisture were calculated by

$$\overline{\theta_{jk}} = \frac{1}{n}\sum_{i=1}^{n}\theta_{ijk} \tag{1}$$

$$\mathrm{Std}_{jk} = \sqrt{\frac{1}{n}\sum\nolimits_{i=1}^{n}\left(\theta_{ijk} - \overline{\theta_{jk}}\right)^2} \tag{2}$$

$$\mathrm{CV}_{jk} = \frac{\mathrm{Std}_{jk}}{\overline{\theta_{jk}}} \tag{3}$$

where θ_{ijk} is the soil moisture for site i at depth k and time j, and n is the number of stations. The arithmetic mean value shown in (1) was used for the SMAP 9 km pixel, while the weighted mean value of the sites was used for the 36 km pixel and the whole study area. In this case, the weighted mean value was calculated by averaging the core validation sites within the 9 km pixel first, and then averaging with other sparse sites.

B. In Situ Network Versus Manual Sampling

Manual ground sampling data provides more dense monitoring of soil moisture in the area. To some extent, the average value of manual sampling points can be closer to the ground truth. However, since the ground sampling campaign was not designed to identify representative sites, some sites had not started recording data during this period [35]. Therefore, only sites S2, S3, S5, S7, and S8 were compared with manual ground sampling data. The daily average soil moisture of each site was compared with the spatial average of manual sampling data in the SMAP 9 km pixel on the same day. The site with the smallest mean absolute deviation was identified as the representative site. The mean absolute error (MAE) is defined as

$$\mathrm{MAE} = \frac{\sum_{j=1}^{D}\left|\overline{\theta_A} - \overline{\theta_B}\right|}{D} \tag{4}$$

where $\overline{\theta_A}$ is the daily average soil moisture at each site and $\overline{\theta_B}$ is the spatial average of the manual ground sampling data. In this study, $D = 7$.

C. Temporal Stability Analysis

The concept of temporal stability was initially introduced by Vachaud et al. [22] and has since been widely utilized in numerous studies to assess the representativeness of monitoring sites [7], [28], [29], [32], [43]. The relative difference (RD) of site i at time j and depth k is defined as

$$\mathrm{RD}_{ijk} = \frac{\theta_{ijk} - \overline{\theta_{jk}}}{\overline{\theta_{jk}}} \tag{5}$$

while the mean relative difference (MRD) and standard deviation of relative difference (SDRD) of site i at depth k can be expressed as

$$\mathrm{MRD}_{ik} = \frac{1}{m}\sum_{j=1}^{m}\mathrm{RD}_{ijk} \tag{6}$$

$$\mathrm{SDRD}_{ik} = \sqrt{\frac{1}{m-1}\sum\nolimits_{j=1}^{m}\left(\mathrm{RD}_{ijk} - \mathrm{MRD}_{ik}\right)^2} \tag{7}$$

where m is the number of observations. The MRD indicates whether each site overestimates or underestimates the mean soil moisture, and the SDRD indicates the temporal stability of each site. Ranking by MRD gives the relative mean soil moisture at each site and assesses the temporal stability of each site. Sites with smaller SDRD are temporally stable sites, which can better capture temporal fluctuations in mean soil moisture and may have some offset from the mean soil moisture.

Grayson and Western [25] proposed that a site exhibiting temporal stability, with a nonzero MRD, could represent the areal average soil moisture if the offset is known. Under the assumption that the MRD remains a constant offset, the estimation of the areal average soil moisture can be expressed as

$$\bar{\theta}_{jk} = \frac{\theta_{ijk}}{1 + \mathrm{MRD}_{ik}} \tag{8}$$

where θ_{ijk} is the soil moisture from temporally stable sites having a nonzero MRD.

Given the temporal stability of the site, the offset (MRD) remains constant and is independent of time. With a simple adjustment, the temporally stable sites can be better used to estimate areal average soil moisture. The method has been well used in subsequent studies [26], [28], [44], [45]. Bias is a potentially correctable problem, while a larger standard deviation is not [17]. Thus, this study considered the site with the smallest SDRD as the representative site. By eliminating the offset between this site and the mean value of all sites, a more accurate estimation of average soil moisture can be achieved using a single site. To evaluate the applicability of Grayson and Western's [25] view to SMN-SDR, this study divided the soil moisture network data into two periods based on date, and conducted temporal stability analysis to identify temporally stable sites. Furthermore, the study also examined whether the offset of representative sites changed.

To mitigate bias caused by an excessive number of stations in a particular area, the arithmetic mean of all stations was employed for the SMAP 9 km pixel, while the same weighted mean as described in Section III-A was used as the ground truth for the 36 km pixel and the entire study area. Temporal stability analysis was conducted for the 9, 36, and 100 km pixel, respectively. Sites were included in the analysis if at least 75% of the data were available, with the exception of sites S1 and L7.

D. Representative Sites Identification

To achieve a similar validation effect to the dense observation network through sparsified ground-based observations, the minimal NRS in the Shandian River basin was determined using random sampling. The root-mean-square error (RMSE)

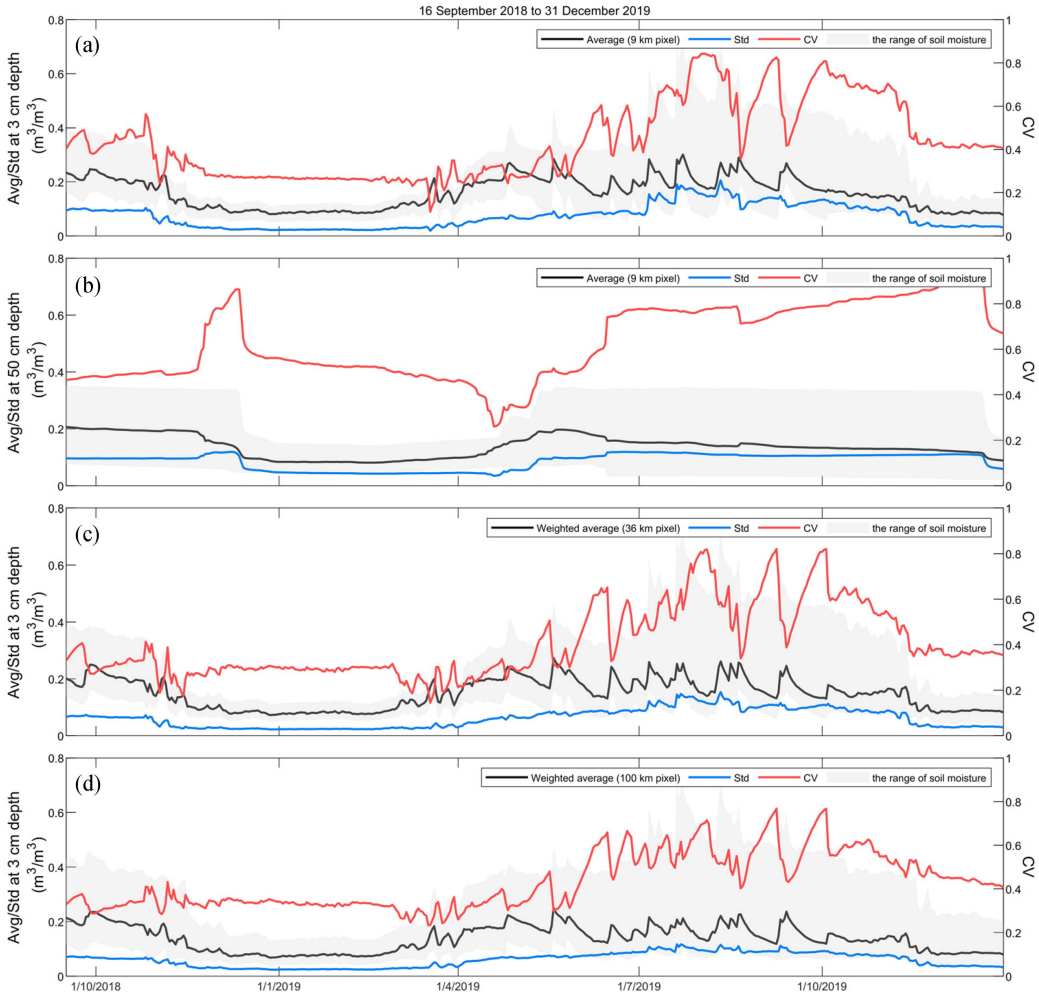

Fig. 2. Temporal variation of the average, Std, and CV of soil moisture at different scales and depths in the Shandian River basin. (a), (c), and (d) 9, 36, and 100 km pixels, respectively, at 3 cm depth. (b) 9 km pixel at 50 cm depth.

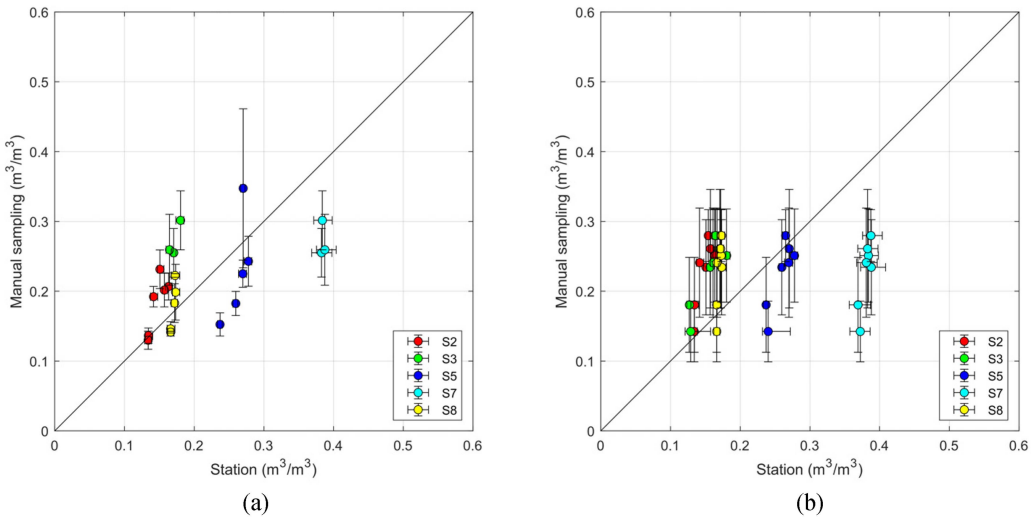

Fig. 3. Comparison of 3 cm site data with manual ground sampling data for SMAP 3 and 9 km pixels. Horizontal error bars: Daily variation of each station. Vertical error bars: Standard deviation of the manual sampling within the pixel.

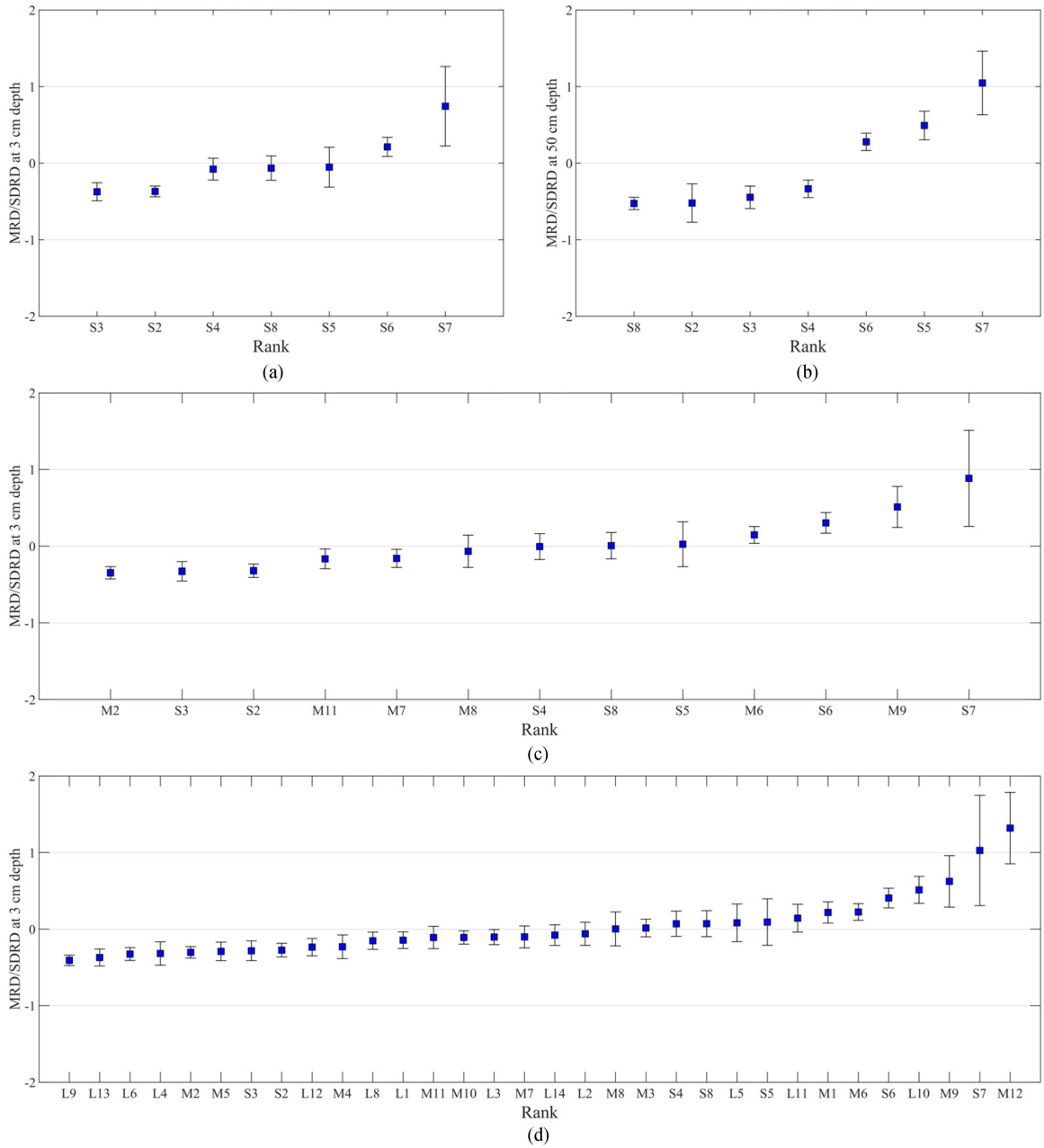

Fig. 4. Temporal stability analysis of sites at different scales and depths in the Shandian River basin. (a), (c), and (d) 9, 36, and 100 km pixels, respectively, at 3 cm depth. (b) 9 km pixel at 50 cm depth. Blue squares: MRD. Black bars: SDRD.

and correlation coefficient (R) were used to quantify differences between sampled sites and all sites. More details of the procedure of random sampling-NRS analysis are in [7] and [29]. Similarly, the RMSE, mean bias (Bias), and correlation coefficient (R), were employed to assess the reliability of the representative sites. These metrics were calculated as follows:

$$\mathrm{RMSE} = \sqrt{\frac{1}{m}\sum_{j=1}^{m}\left(y_j - \overline{\theta_j}\right)^2} \tag{9}$$

$$\mathrm{Bias} = \frac{1}{m}\sum_{j=1}^{m}\left(y_j - \overline{\theta_j}\right) \tag{10}$$

$$\mathrm{R} = \frac{\sum_{i=1}^{m}\left(y_j - \overline{y}\right)\left(\overline{\theta}_j - \overline{\theta}\right)}{\sqrt{\sum_{i=1}^{m}\left(y_j - \overline{y}\right)\sum_{i=1}^{N}\left(\overline{\theta}_j - \overline{\theta}\right)}} \tag{11}$$

where y_j is the areal average soil moisture estimated by the representative stations at time j, and $\overline{\theta_j}$ is the measured average soil moisture at time j.

E. SMAP Soil Moisture Products Validation

Prior to the validation process, quality control procedures were implemented for the SMAP soil moisture products. Due to the limited availability of usable data for SMAP L2 data (SPL2SMAP_S), no quality control was applied, and all

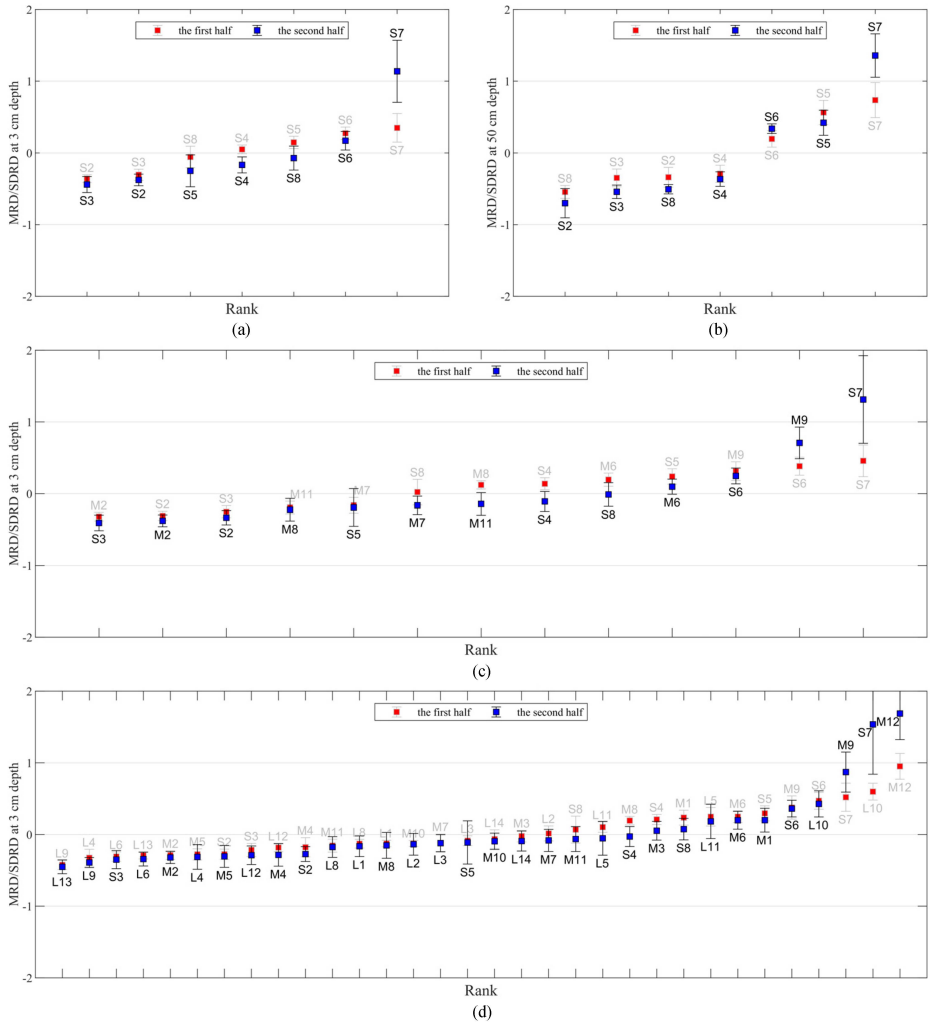

Fig. 5. Temporal stability analysis of sites at different scales and depths in the Shandian River basin. (a), (c), and (d) 9, 36, and 100 km pixels, respectively, at 3 cm depth. (b) 9 km pixel at 50 cm depth. Red square: MRD of the former period; Blue square: MRD of the latter period; Black error bar: SDRD.

data were used for validation. Regarding the SMAP L3 data (SPL3SMP_E and SPL3SMP), only data flagged as "Soil moisture retrieval has recommended quality" were used [46]. As for the SMAP L4 data (SPL4SMGP), direct validation was conducted since no quality flag was available.

Considering the presence of frozen soil in the Shandian River basin, soil moisture data from sites with soil temperatures below 273.15 K were excluded. Representative sites at depths of 3 and 50 cm were used to estimate the areal average soil moisture, which were then used to validate the SMAP surface soil moisture products (SPL2SMAP_S, SPL3SMP_E, SPL3SMP, SPL4SMGP) and root zone soil moisture product (SPL4SMGP). Four statistical metrics, namely, RMSE, unbiased RMSE (ubRMSE), mean bias (Bias), and correlation coefficient (R), were employed to comprehensively assess the accuracy of the SMAP soil moisture products using *in situ* data that corresponded to the observed time of the respective SMAP soil moisture products [47]. The influence of changes in the number of stations on the validation of soil moisture products was also analyzed.

IV. Results and Discussion

A. Spatiotemporal Variability of Soil Moisture

Fig. 2 illustrates the temporal dynamics of daily average soil moisture across three spatial scales (9, 36, 100 km) and two depths (3, 50 cm) in the Shandian River basin, spanning from September 16, 2018 to December 31, 2019. In addition, the spatial variability of soil moisture is described through the utilization of the Std and CV calculated from the soil moisture data.

The three variables (Avg, Std, and CV) exhibited distinct seasonal variations at different scales and depths. Specifically, at the 3 cm depth, the average soil moisture in the Shandian River basin ranged from 0.07 to 0.30 m^3/m^3 across the three scales. Soil moisture showed higher values during the summer and lower values during the winter, with substantial changes occurring during the freeze-thaw season. It should be noted that due to the presence of freezing conditions in the basin, the instruments were only able to detect liquid water, resulting in consistently low soil moisture observations during the winter and consequently a lower coefficient of variation among the sites.

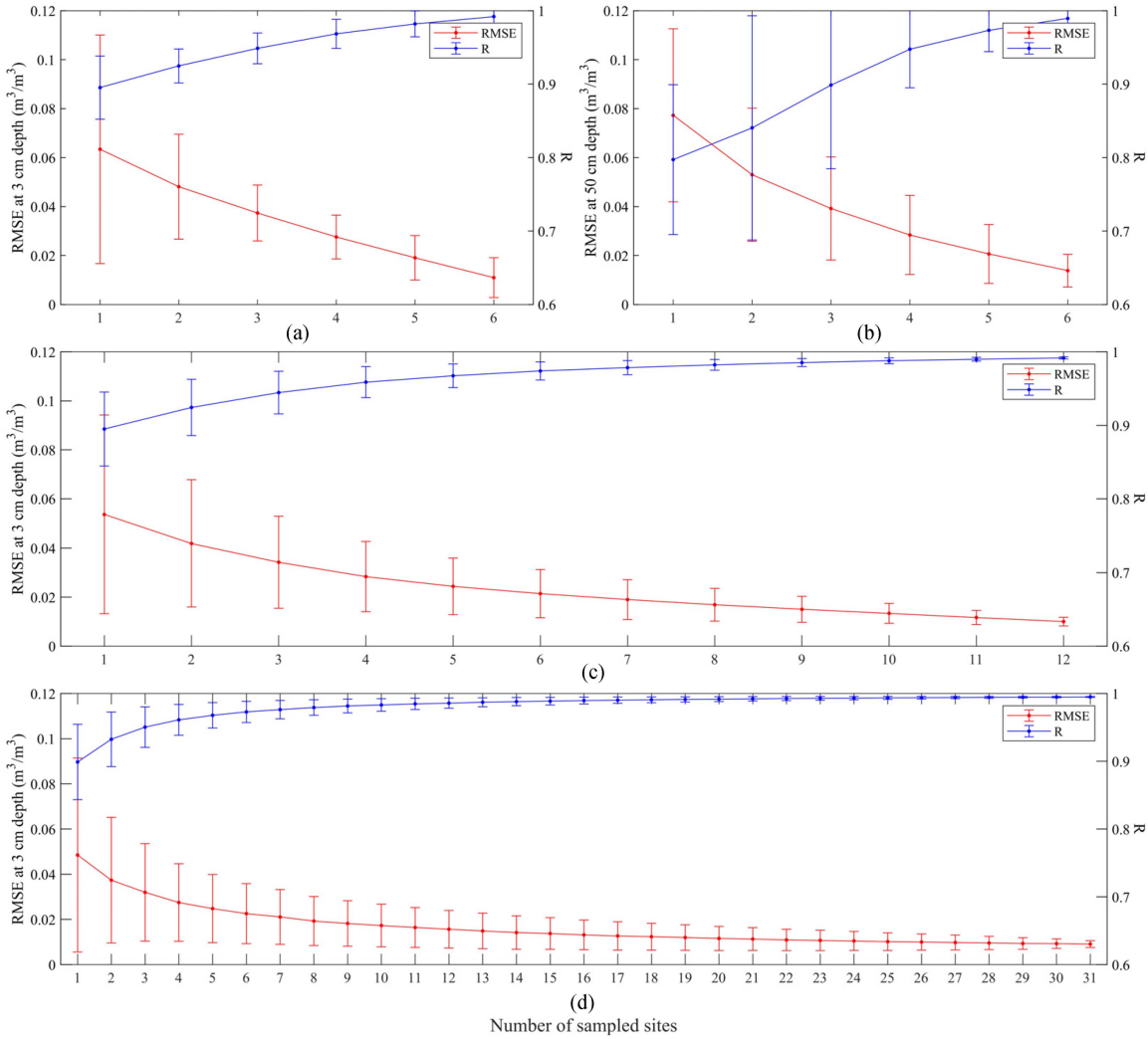

Fig. 6. Variation of RMSE and R with the number of sampled sites at different scales and depths in the Shandian River basin. (a), (c), and (d) 9, 36, and 100 km pixels, respectively, at 3 cm depth. (b) 9 km pixel at 50 cm depth.

In contrast, during the summer, soil moisture exhibited greater fluctuations due to the influence of rainfall and irrigation. The variability in soil moisture was further exacerbated by variations in land types and vegetation cover, leading to notable differences in soil moisture among different sites and resulting in a higher CV. While the Std captures the overall variability of soil moisture, the normalized CV is more suitable for describing the relative variability of soil moisture, as it takes into account the average soil moisture value. This is consistent with previous studies that have highlighted the utility of CV in characterizing soil moisture dynamics [7], [29]. Moreover, this study found that the CV, compared to the Std, better captured the seasonal variation of soil moisture. By normalizing the variability with respect to the average, the CV provides a more comprehensive understanding of the relative changes in soil moisture throughout the seasons. Overall, the analysis of Avg, Std, and CV reveals the spatiotemporal dynamics of soil moisture in the Shandian River basin, highlighting the influence of seasonal variations, freeze-thaw cycles, and land characteristics on soil moisture patterns.

Crow et al. [14] highlighted that both the Std and CV of soil moisture increase with increasing spatial scale. In the study, the minimum values of Std and CV of soil moisture increased with scale, while the maximum values decreased, although the overall changes were not substantial. The maximum and minimum values of average soil moisture decreased with scale, mainly due to the higher soil moisture observed at site S7 in the 9 km pixel relative to other sites. As the number of sites increased, the weighted average of all sites tended to stabilize. This suggests that sparse sites are likely to include more dry sites compared to the core validation sites. Within the 9 km pixel, temporal changes in Avg and Std at the 50 cm depth were smaller compared to the 3 cm depth. However, the CV exhibited more complex changes and greater variability among different sites. Overall, the spatial heterogeneity of soil moisture in the Shandian River basin was not substantially affected by changes in spatial scale, but it showed a substantial increase with increasing depth in the vertical direction. The findings indicate that the spatial heterogeneity of soil moisture in the Shandian River basin was influenced by both spatial scale and vertical depth [42], [48]. The

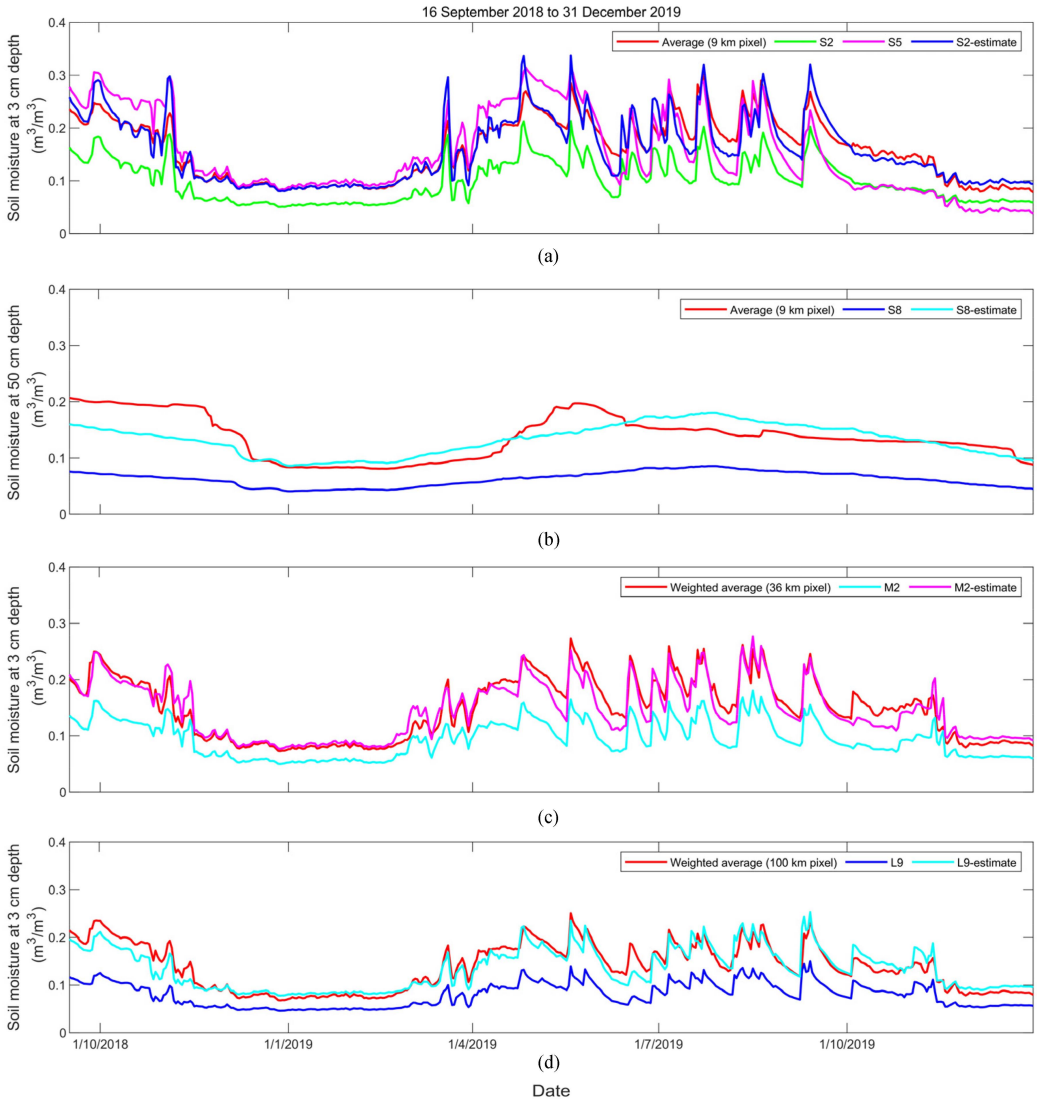

Fig. 7. Time series of soil moisture representative sites in the Shandian River basin at different scales and depths. (a), (c), (d) 9, 36, and 100 km pixels, respectively, at 3 cm depth. (b) 9 km pixel at 50 cm depth.

observed patterns of soil moisture variability provide valuable insights into the dynamics of soil moisture distribution, which is crucial for understanding hydrological processes in the study area.

B. In Situ Network Versus Manual Sampling

The representativeness of different sites was assessed using manual ground sampling data. Fig. 3 depicts the daily variations at each site using horizontal bars, while the vertical bars illustrate the standard deviation of the manual sampling data within the corresponding SMAP pixel.

According to Fig. 3, sites S2 and S3 (S7) consistently show lower (higher) soil moisture levels compared to the manual ground sampling data for both the SMAP 3 and 9 km pixels.

The differences indicate potential biases or discrepancies between the sampled data and the corresponding SMAP soil moisture products. In addition, the spatial variability of soil moisture in the 9 km pixel is greater than the temporal variability, as observed in Fig. 3. This can be attributed to the heterogeneous land use patterns in the Shandian River basin, which lead to pronounced spatial variations in soil moisture rather than temporal variations [32].

Sites S2, S3, S5, S7, and S8 correspond to different SMAP 3 km pixels. Among these sites, S2 and S8 exhibited smaller MAE for the SMAP 3 km pixels, with values of 0.038 and 0.026 m^3/m^3, respectively. However, it should be noted that the 3 km pixel containing S8 had relatively few manual sampling points, resulting in a higher level of uncertainty in the data. Therefore, S2 was identified as the representative site for the SMAP 3 km pixel, considering its lower MAE and relatively more robust sampling coverage.

For the 9 km pixel, the average MAE of all sites with manual ground sampling data was 0.039 m^3/m^3, indicating a relatively even distribution of sites that can effectively represent the areal average soil moisture. Among these sites, S5 exhibited the smallest MAE of 0.037 m^3/m^3 for the 9 km pixel, making it the selected representative site for this pixel.

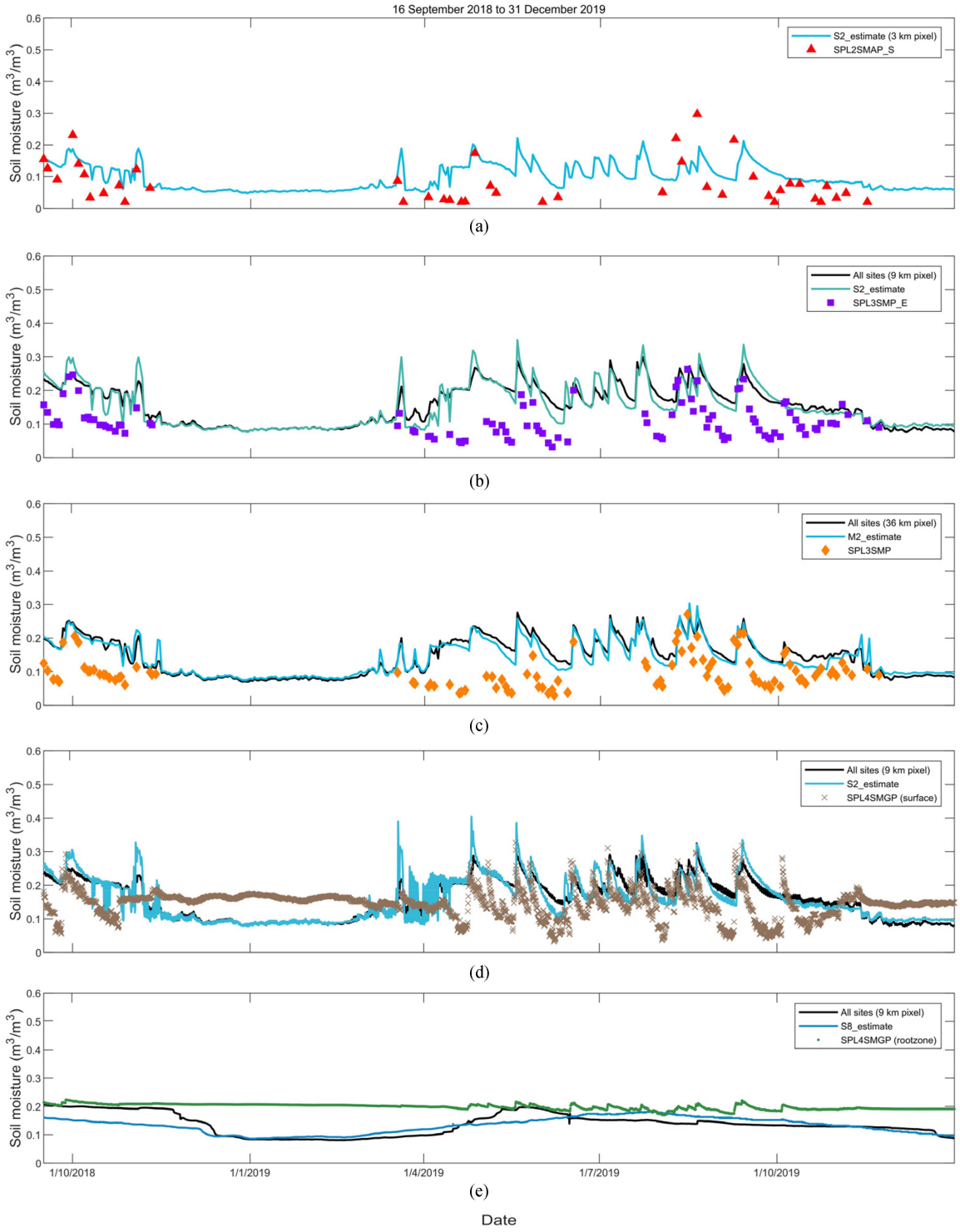

Fig. 8. Time series comparison of *in situ* soil moisture and SMAP L2, L3, and L4 soil moisture products in the Shandian River basin. (a) SPL2SMAP_S soil moisture product, (b) SPL3SMP_E soil moisture product, (c) SPL3SMP soil moisture product, (d) SPL4SMGP soil moisture product (surface), (e) SPL4SMGP soil moisture product (root zone).

Directly selecting representative sites solely based on MAE may not guarantee their ability to accurately capture the variability of areal average soil moisture. The limited time series of manual ground sampling data may not ensure the representativeness of the selected sites in other periods. Therefore, it is important to acknowledge the limitations of the current study and emphasize the need for more intensive and extensive sampling data in the future to obtain more reliable and robust conclusions.

C. Temporal Stability Analysis

Temporal stability analysis was performed on the soil moisture data obtained from SMN-SDR at the 9, 36, and 100 km pixel

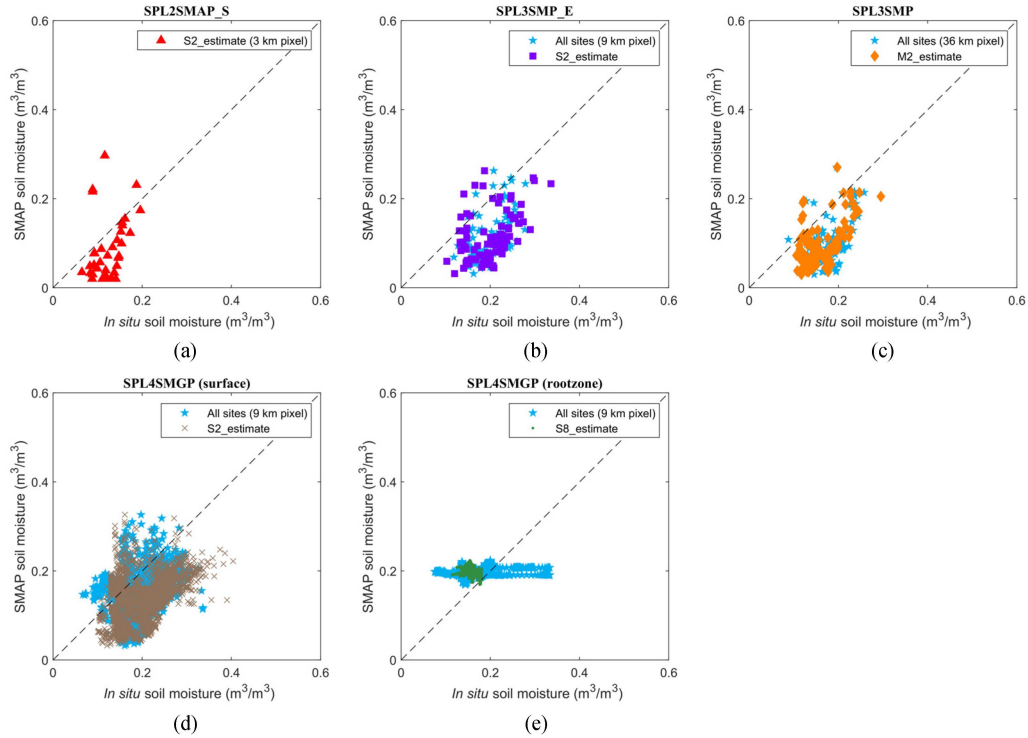

Fig. 9. Scatter plots of *in situ* soil moisture and SMAP L2, L3, and L4 soil moisture products in the Shandian River basin. (a) SPL2SMAP_S soil moisture product, (b) SPL3SMP_E soil moisture product, (c) SPL3SMP soil moisture product, (d) SPL4SMGP soil moisture product (surface), and (e) SPL4SMGP soil moisture product (root zone).

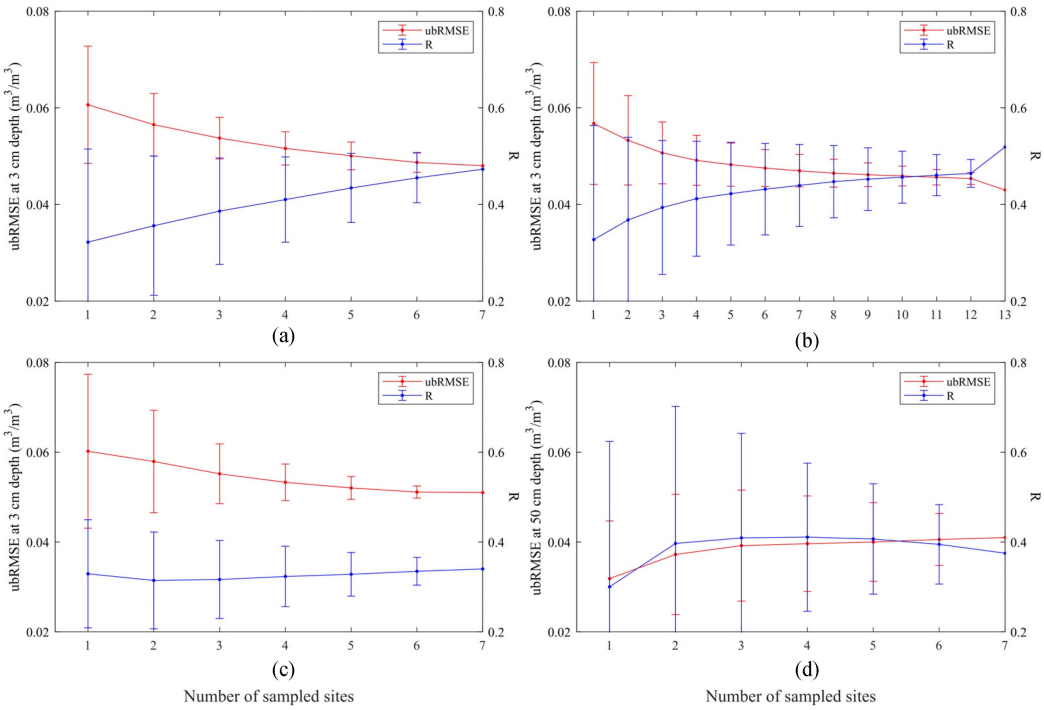

Fig. 10. Variation of ubRMSE and R of *in situ* soil moisture and SMAP L3 and L4 soil moisture products with the number of sampled sites at different scales and depths in the Shandian River basin. (a) SPL3SMP_E soil moisture product, (b) SPL3SMP soil moisture product, (c) SPL4SMGP soil moisture product (surface), and (d) SPL4SMGP soil moisture product (root zone).

TABLE I
REPRESENTATIVE STATIONS BASED ON DIFFERENT METHODS FOR EACH PIXEL

Pixel	Method of identification		
	Temporal stability		Manual sampling
	MRD	SDRD	MAE
3 km	–	–	S2
9 km	S5(S6)	S2(S8)	S5
36 km	S8	M2	–
100 km	M8	L9	–

scales. Fig. 4 presents the ranking of each site based on the MRD, from the smallest to the largest value, to assess whether each site tended to overestimate or underestimate the areal average soil moisture. The standard deviation of the relative difference (SDRD) was used as an indicator of the temporal stability of each site. Table I provides a summary of the representative sites selected using different criteria.

The range of MRD and SDRD increased with larger scales due to the considerable variability in soil types and vegetation cover [49]. Fig. 4 illustrates that the average MRD and SDRD values for the 3 cm depth showed no obvious variation across different scales. However, for the 50 cm depth within the 9 km pixel, the average MRD was notably higher than that for the 3 cm depth, indicating greater spatial heterogeneity of soil moisture at the 50 cm depth. Importantly, it is worth noting that despite the use of different indicators, the same conclusions as in Section IV-A were consistently reached.

According to Fig. 4(a), site S2 and S3 (S7) notably underestimated (overestimated) the areal average soil moisture at a depth of 3 cm within the 9 km pixel. Among the sites, S5 exhibited the smallest difference from the average soil moisture, with an MRD of −0.051. Comparatively, S2 had a smaller SDRD than S5, making it the most representative site in the 9 km pixel at a depth of 3 cm. Therefore, S2 was better suited to capture the temporal variation of the average soil moisture.

As depicted in Fig. 4(b), at a depth of 50 cm, none of the sites had an MRD close to zero. Similarly, the site with the smallest SDRD, S8, was selected as the representative site. The complexity of the soil structure leads to different representative sites at different depths. In comparison to the 3 cm depth, the MRD and SDRD of different sites at the 50 cm depth exhibited noteworthy changes. However, sites S6 and S7 (S2) consistently overestimated (underestimated) the areal average soil moisture at both depths.

As illustrated in Fig. 4(c)–(d), for the 36 and 100 km pixels, sites S8 and M8 exhibited small MRD values of 0.004 and 0.003, respectively. Furthermore, the sites with the smallest SDRD values were M2 and L9, respectively. The similarity in soil moisture variability observed at different scales within the 3 cm depth suggests that certain sites exhibit temporal stability at a small scale that is maintained at larger scales. Specifically, S2 demonstrated a small SDRD at the 9 km pixel, while M2 displayed a small SDRD at the 36 km pixel. In addition, both S2 and M2 maintained a small SDRD at the 100 km pixel. Conversely, site M12 overestimated the average soil moisture by 131.95%, while site S7 consistently overestimated soil moisture at all three scales and two depths, showing poor temporal stability. Although the temporal stability analysis suggests poor representativeness for these sites, this study recognizes that these sites may capture soil moisture information that was not captured by other sites.

There is no universally accepted standard for identifying representative sites using temporal stability analysis. Different indicators may lead to different representative sites, and so it is essential to choose indicators based on specific requirements. Generally, relatively dry sites tend to have smaller SDRD values, indicating better temporal stability [7], [43]. From Fig. 4(a)–(d), it can be observed that the representative sites S2, S8, M2, and L9 consistently underestimated the areal average soil moisture at different scales and depths. This may be attributed to the fact that these sites exhibit less variability, and so capture the temporal variation of average soil moisture more effectively. The use of SDRD as a selection indicator for representative sites is particularly advantageous for these dry sites. Since there is an offset between these stations and the average soil moisture, a direct validation of the remote sensing soil moisture product would lead to an overestimation of the validation results. Therefore, the offset needs to be corrected using (8) to ensure accurate validation.

To further verify the reliability of these representative sites and explain the variation pattern of each site during different seasons. The soil moisture site data utilized in this study were divided into two periods based on date: September 16, 2018 to May 10, 2019, and May 11, 2019 to December 31, 2019. This division allowed for a separate temporal stability analysis of each site in the two periods, enabling a comprehensive assessment of their temporal behavior. As depicted in Fig. 5, the MRD and SDRD of the sites exhibited remarkable changes between the two periods. This variation can be attributed to the difference in seasonal conditions, with the latter period having fewer freezing period data and a higher proportion of summer data compared to the first period. Consequently, the spatial variability among different sites was more pronounced in the latter period. The seasonal influence resulted in distinct characteristics of the sites in different periods.

At 3 cm depth and various scales, site S5 exhibited overestimation in the former period and underestimation in the latter period. In contrast, sites S2 and S3 consistently underestimated the average soil moisture across all three scales and two depths in both periods. Sites S6 and S7 consistently overestimated the average soil moisture. Notably, compared to the former period, sites S7 and M12 exhibited a greater deviation from the average soil moisture, suggesting that these sites were more responsive to rainfall and irrigation activities in the area.

Due to the strong spatial heterogeneity of soil moisture, only specific sites can maintain temporal stability [25]. As observed in Fig. 5(a)–(d), the MRD of sites S2, S8, M2, and L9 did not exhibit remarkable changes. In addition, the SDRD for these sites remained consistently low, indicating that the offsets between these sites and the mean value did not vary notably and maintained temporal stability over the study period. Throughout the entire study period, sites S2, S8, M2, and L9 consistently

TABLE II
NRS AND SPECIFIC SITES OF SMN-SDR

Pixel	Depth (cm)	NRS	Sites	R/RMSE (m^3/m^3)
9 km	3	5	S2, S3, S5, S7, S8	0.9963/0.0065
9 km	50	6	S2, S3, S4, S5, S7, S8	0.9956/0.0063
36 km	3	7	M2, M6, M7, M8, M9, M11, S6	0.9984/0.0042
100 km	3	8	L2, L5, L8, L11, L14, M1, M2, M3	0.9956/0.0047

underestimated the average soil moisture, with relative underestimations of 36.83%, 52.57%, 34.79%, and 40.69%, respectively. These underestimations exhibited temporal stability, as reflected by the small SDRD values of 0.0696, 0.0804, 0.0783, and 0.0689, respectively.

Grayson and Western [25] highlighted that, due to the temporal stability of these sites, the offset remains constant regardless of the time of year. By making a simple adjustment based on these sites, a more accurate estimation of the areal average soil moisture can be achieved [28]. Similarly, this study reached similar conclusions. Therefore, in the context of this study, the temporally stable sites S2, S8, M2, and L9 were selected as the most representative sites at two depths and three scales within the Shandian River basin. To improve the estimation of the areal average soil moisture, the offset of the representative sites needed to be corrected. By incorporating this correction, a more reliable relationship between the representative sites and the areal average could be established. The corrected relationship can be expressed as

$$\mathrm{SM}_{9\mathrm{km}} = \frac{\mathrm{SM}_{\mathrm{S2}}}{0.6317}(3\,\mathrm{cm\ depth}) \tag{12}$$

$$\mathrm{SM}_{9\mathrm{km}} = \frac{\mathrm{SM}_{\mathrm{S8}}}{0.4743}(50\,\mathrm{cm\ depth}) \tag{13}$$

$$\mathrm{SM}_{36\mathrm{km}} = \frac{\mathrm{SM}_{\mathrm{M2}}}{0.6521}(3\,\mathrm{cm\ depth}) \tag{14}$$

$$\mathrm{SM}_{100\mathrm{km}} = \frac{\mathrm{SM}_{\mathrm{L9}}}{0.5931}(3\,\mathrm{cm\ depth}). \tag{15}$$

D. Representative Sites Assessment

Fig. 6 shows the variation of RMSE and R with the number of sampling sites at multiple scales and depths in the Shandian River basin. Table II provides the minimal NRS and specific sites for a given accuracy of RMSE < 0.02 m^3/m^3, R > 0.95. As shown in Fig. 6(a)–(d), both RMSE and R maintain opposite trends as the number of sampling sites increases, regardless of scale and depth. In particular, Fig. 6(d) clearly illustrates that site increase up to a certain level of accuracy remains relatively stable. Thus, the specific site combinations and the minimal NRS presented in Table II provide a reference for the subsequent establishment and maintenance of the network in the region.

TABLE III
RMSE, BIAS, AND R BETWEEN ESTIMATED AVERAGE SOIL MOISTURE OF REPRESENTATIVE SITES AND MEASURED AVERAGE SOIL MOISTURE

Pixel	Site	RMSE (m^3/m^3)	Bias (m^3/m^3)	R
9 km (3 cm)	S5	0.041	–0.005	0.860
9 km (3 cm)	S2-estimate	0.020	0.000	0.945
9 km (50 cm)	S8-estimate	0.028	–0.005	0.695
36 km (3 cm)	M2-estimate	0.018	–0.003	0.946
100 km (3 cm)	L9-estimate	0.017	–0.003	0.936

Fig. 7 presents a time series comparison between the estimated average soil moisture and the measured average soil moisture for representative sites at various scales and depths in the Shandian River basin, spanning from September 16, 2018 to December 31, 2019. Table III provides the corresponding RMSE, Bias, and R values, quantifying the differences between the estimated areal average soil moisture and the measured average soil moisture.

Through a comparison, it was observed that within the 9 km pixel, site S2 (based on SDRD) outperformed site S5 (based on MAE and MRD) in estimating the areal average soil moisture at a depth of 3 cm. This further supports the feasibility of utilizing this method for identifying representative sites. As depicted in Fig. 6, the sites with the lowest SDRD values at different scales and at a depth of 3 cm can effectively estimate the areal average soil moisture by correcting the offset using (12)–(15). However, due to the limited temporal variation of average soil moisture at a depth of 50 cm and the significant spatial heterogeneity among sites, it becomes difficult to identify a representative site at this depth using temporal stability analysis. Consequently, the selected representative site exhibits a poor correlation with the mean value. Since the representative site within the 3 km pixel could only be determined by comparing it with the manual ground sampling data, S2 was identified as the representative site in the 3 km pixel. At a depth of 3 cm, for the 9 and 36 km pixels, the estimated average soil moisture from sites S2 and M2 exhibited high accuracy and correlation with the measured average values, with an RMSE of 0.020 and 0.018 m^3/m^3, and an R value of 0.945 and 0.946, respectively. While it cannot be guaranteed that representative sites can fully replace all sites, using only representative sites yielded results similar to using all [21]. In the next section, the estimated average soil moisture obtained from the identified representative sites will be utilized as *in situ* soil moisture data to validate the SMAP soil moisture products.

E. SMAP Soil Moisture Products Validation

To validate the SMAP soil moisture products, the soil moisture estimated from the representative sites was considered as the reference value at the pixel scale, following the approach used by Yee et al. [21], and all sites were also used to compare. Figs. 8 and 9 present the time series and scatter plots for validation using representative sites and all sites, respectively. Table IV summarizes the validation results for representative sites and all sites.

TABLE IV
VALIDATION RESULTS FOR REPRESENTATIVE SITES AND ALL SITES

		Depth (cm)	RMSE (m^3/m^3)	ubRMSE (m^3/m^3)	Bias (m^3/m^3)	R	N
SPL2SMAP_S	All sites	3	–	–	–	–	–
	S2_eatimate		0.076	0.066	–0.038	0.342	37
SPL3SMP_E	All sites		0.100	0.048	–0.088	0.473	99
	S2_estimate		0.100	0.054	–0.084	0.439	88
SPL3SMP	All sites		0.091	0.043	–0.080	0.519	100
	M2_estimate		0.081	0.044	–0.068	0.529	99
SPL4SMGP (surface)	All sites		0.077	0.051	–0.058	0.340	2357
	S2_estimate		0.083	0.055	–0.063	0.397	2230
SPL4SMGP (root zone)	All sites	50	0.050	0.041	0.028	0.375	2827
	S8_estimate		0.052	0.022	0.048	–0.288	2420

As shown in Fig. 9(a)–(c) and Table IV, the bias of SMAP L2 and L3 products compared to representative sites soil moisture data ranged from -0.084 to -0.038 m^3/m^3, the ubRMSE ranged from 0.044 to 0.066 m^3/m^3, and R ranged from 0.342 to 0.529. At all three scales, SMAP L2 and L3 products exhibited an underestimation of surface soil moisture. It is worth noting that previous studies validating SMAP products using the mean values of stations have also reported accuracy issues with SMAP soil moisture products [12]. The SPL3SMP soil moisture product exhibits higher R compared to both the SPL2SMAP_S and SPL3SMP_E soil moisture products, and it also has a smaller ubRMSE. Due to the impact of vegetation cover on satellite observations, Nadeem et al. [2] also found poor performance of the SPL3SMP_E product in previous validations, which was confirmed in this study. As shown in Fig. 9(d)–(e) and Table IV, the R and Bias for the SPL4SMGP surface soil moisture product using the representative site were relatively low compared to the SPL3SMP_E surface soil moisture product, and the ubRMSE were similar for both products. Despite this, the L4 product did not exhibit better performance than the L3 product, which could be attributed to the poor performance of SMAP at this scale and the limited availability of L3 data. On the other hand, the SPL4SMGP root zone soil moisture product tended to overestimate soil moisture relative to the *in situ* measurements.

The validation results for the representative site, and all sites, are relatively similar for the SMAP surface soil moisture products, as shown in Fig. 9(b)–(d) and Table IV. Given the notable variation in soil moisture at a depth of 50 cm and the limited number of stations, it is possible that the selected representative sites may not effectively capture the temporal changes in areal average soil moisture, resulting in negative R values. Therefore, it is recommended to employ multiple sites for validation purposes at this depth.

Fig. 10 illustrates the relationship between the number of sites and the validation metric (ubRMSE, R) for SMAP products. In general, the validation accuracy improved with an increasing number of sites, as depicted in Fig. 10(a)–(c) for the three SMAP surface soil moisture products. However, for the SMAP root zone soil moisture product, ubRMSE increases with the number of sites, and R exhibited an initial increase followed by a decrease. This phenomenon may be attributed to the high spatial variability at this depth, which made it challenging to obtain dependable validation results for a few sites.

In summary, different SMAP soil moisture products exhibited notable underestimation of surface soil moisture in SMN-SDR, and none of them met the expected accuracy of ubRMSE less than 0.04 m^3/m^3. Moreover, SMAP soil moisture products overestimated root zone soil moisture. These findings can be attributed to various factors. First, the study area, the Shandian River basin, is situated in an agricultural irrigation region, and the limited revisit period of SMAP may hinder its ability to capture irrigation events in a timely manner. Second, the construction of the SMN-SDR may have involved some compromise between scientific validity and operability, and the stations themselves may not reflect the spatial pattern of areal soil moisture well, leading to insufficient spatial representativeness of the selected stations through time stability analysis. Further optimization of station design may be beneficial for addressing this issue. However, when it comes to the SMAP surface soil moisture products, the validation results from the representative sites closely align with those from all the sites.

V. CONCLUSION

This study employed SMN-SDR soil moisture data and manual ground sampling data to analyze the spatiotemporal variability of soil moisture in the Shandian River basin from multiple perspectives. The study demonstrated the feasibility of utilizing representative sites for estimating watershed-average soil moisture and evaluating satellite remote sensing soil moisture products. Based on the analysis, the following conclusions were drawn.

1) The spatial heterogeneity of soil moisture in the Shandian River basin does not exhibit notable variation with changing scale but shows a noticeable increase with depth and seasonal variations. The strategically selected core validation sites of SMN-SDR were adequately distributed and effectively represented the average soil moisture of the area. However, the sparse sites mainly represent dry

areas, which can result in discrepancies between their mean values and the ground truth.

2) By conducting temporal stability analysis, representative sites were successfully identified at various scales and depths that exhibited consistent temporal stability across different time periods. Specifically, at a depth of 3 cm, the selected representative sites demonstrated high accuracy and a strong correlation between the estimated average soil moisture and the measured average soil moisture. This provides valuable insights for estimating areal average soil moisture, and validating satellite data in future studies.
3) The SMAP soil moisture products underestimated surface soil moisture and failed to meet the desired accuracy criterion of ubRMSE < 0.04 m^3/m^3. Conversely, SMAP overestimated root zone soil moisture. Among the SMAP products used, the SMAP L3 36 km soil moisture product (SPL3SMP) showed the highest correlation with the SMN-SDR stations.

This study focused on assessing the reliability of the selected representative sites within the study period. Future research should investigate whether the selected representative sites remain valid under varying vegetation conditions. The well-distributed monitoring stations demonstrated their effectiveness in monitoring soil moisture changes spatially. Therefore, for future network design, it is recommended to consider representative stations at different depths and scales for a more comprehensive and reasonable layout. The findings of this study contribute to the theoretical understanding of estimating soil moisture at the watershed scale and provide a scientific basis for optimizing the design of soil moisture networks in watersheds.

ACKNOWLEDGMENT

The authors would like to express gratitude to soil moisture experiment in the Luan River for generously providing their data, which enabled to conduct the study.

REFERENCES

[1] V. Humphrey et al., "Soil moisture-atmosphere feedback dominates land carbon uptake variability," *Nature*, vol. 592, no. 7852, pp. 65–69, Apr. 2021.
[2] A. A. Nadeem et al., "Multi-scale assessment of SMAP level 3 and level 4 soil moisture products over the soil moisture network within the ShanDian River (SMN-SDR) Basin, China," *Remote Sens.*, vol. 14, no. 4, p. 982, Feb. 2022.
[3] C. Yi et al., "Assessment of five SMAP soil moisture products using ISMN ground-based measurements over varied environmental conditions," *J. Hydrol.*, vol. 619, 2023, Art. no. 129325.
[4] E. Pinnington et al., "Improving soil moisture prediction of a high-resolution land surface model by parameterising pedotransfer functions through assimilation of SMAP satellite data," *Hydrol. Earth System Sci.*, vol. 25, no. 3, pp. 1617–1641, 2021.
[5] L. Vilasa, D. G. Miralles, R. A. M. de Jeu, and A. J. Dolman, "Global soil moisture bimodality in satellite observations and climate models," *J. Geophysical Res.-Atmospheres*, vol. 122, no. 8, pp. 4299–4311, Apr. 2017.
[6] C. Wang, B. Fu, L. Zhang, and Z. Xu, "Soil moisture-plant interactions: An ecohydrological review," *J. Soils Sediments, Rev.*, vol. 19, no. 1, pp. 1–9, Jan. 2019.
[7] J. Chen, J. Wen, and H. Tian, "Representativeness of the ground observational sites and up-scaling of the point soil moisture measurements," *J. Hydrol.*, vol. 533, pp. 62–73, 2016.
[8] J. Peng et al., "The impact of the Madden-Julian Oscillation on hydrological extremes," *J. Hydrol.*, vol. 571, pp. 142–149, 2019.
[9] S. Zhou et al., "Land-atmosphere feedbacks exacerbate concurrent soil drought and atmospheric aridity," *Proc. Nat. Acad. Sci. United States Amer.*, vol. 116, no. 38, pp. 18848–18853, Sep. 2019.
[10] C. S. Kang et al., "Global soil moisture retrievals from the Chinese FY-3D microwave radiation imager," *IEEE Trans. Geosci. Remote Sens.*, vol. 59, no. 5, pp. 4018–4032, May 2021.
[11] J. Peng, A. Loew, O. Merlin, and N. E. C. Verhoest, "A review of spatial downscaling of satellite remotely sensed soil moisture," *Rev. Geophys.*, vol. 55, no. 2, pp. 341–366, 2017.
[12] J. Zheng et al., "Assessment of 24 soil moisture datasets using a new in situ network in the Shandian River Basin of China," *Remote Sens. Environ.*, vol. 271, 2022, Art. no. 112891.
[13] J. P. Wigneron et al., "Modelling the passive microwave signature from land surfaces: A review of recent results and application to the L-band SMOS & SMAP soil moisture retrieval algorithms," *Remote Sens. Environ.*, vol. 192, pp. 238–262, Apr. 2017.
[14] W. T. Crow et al., "Upscaling sparse ground-based soil moisture observations for the validation of coarse-resolution satellite soil moisture products," *Rev. Geophys.*, vol. 50, 2012, Art. no. 2.
[15] J. Whitcomb et al., "Evaluation of SMAP core validation site representativeness errors using dense networks of in situ sensors and random forests," *IEEE J. Sel. Topics Appl. Earth Observ. Remote Sens.*, vol. 13, pp. 6457–6472, 2020.
[16] W. G. Brown, M. H. Cosh, J. Dong, and T. E. Ochsner, "Upscaling soil moisture from point scale to field scale: Toward a general model," *Vadose Zone J.*, vol. 22, 2023, Art. no. e20244.
[17] M. H. Cosh, T. J. Jackson, P. Starks, and G. Heathman, "Temporal stability of surface soil moisture in the Little Washita River watershed and its applications in satellite soil moisture product validation," *J. Hydrol.*, vol. 323, no. 1–4, pp. 168–177, 2006.
[18] D. Kathuria, B. P. Mohanty, and M. Katzfuss, "A nonstationary geostatistical framework for soil moisture prediction in the presence of surface heterogeneity," *Water Resour. Res.*, vol. 55, no. 1, pp. 729–753, Jan. 2019.
[19] X. Cai et al., "Validation of SMAP soil moisture for the SMAPVEX15 field campaign using a hyper-resolution model," *Water Resour. Res.*, vol. 53, no. 4, pp. 3013–3028, Apr. 2017.
[20] S. Gao, Z. Zhu, H. Weng, and J. Zhang, "Upscaling of sparse in situ soil moisture observations by integrating auxiliary information from remote sensing," *Int. J. Remote Sens.*, vol. 38, no. 17, pp. 4782–4803, 2017.
[21] M. S. Yee, J. P. Walker, C. Rüdiger, R. M. Parinussa, T. Koike, and Y. H. Kerr, "A comparison of SMOS and AMSR2 soil moisture using representative sites of the OzNet monitoring network," *Remote Sens. Environ.*, vol. 195, pp. 297–312, 2017.
[22] G. Vachaud, A. Passerat de Silans, P. Balabanis, and M. Vauclin, "Temporal stability of spatially measured soil water probability density function," *Soil Sci. Soc. Amer. J.*, vol. 49, no. 4, pp. 822–828, 1985.
[23] G. Singh, R. K. Panda, and B. P. Mohanty, "Spatiotemporal analysis of soil moisture and optimal sampling design for regional-scale soil moisture estimation in a tropical watershed of India," *Water Resour. Res.*, vol. 55, no. 3, pp. 2057–2078, Mar. 2019.
[24] E. J. Coopersmith et al., "Understanding temporal stability: A long-term analysis of USDA ARS watersheds," *Int. J. Digit. Earth*, vol. 14, no. 10, pp. 1243–1254, Oct. 2021.
[25] R. B. Grayson and A. W. Western, "Towards areal estimation of soil water content from point measurements: Time and space stability of mean response," *J. Hydrol.*, vol. 207, no. 1/2, pp. 68–82, 1998.
[26] G. C. Heathman, M. H. Cosh, E. Han, T. J. Jackson, L. McKee, and S. McAfee, "Field scale spatiotemporal analysis of surface soil moisture for evaluating point-scale in situ networks," *Geoderma*, vol. 170, pp. 195–205, 2012.
[27] Y. Ran, X. Li, R. Jin, J. Kang, and M. H. Cosh, "Strengths and weaknesses of temporal stability analysis for monitoring and estimating grid-mean soil moisture in a high-intensity irrigated agricultural landscape," *Water Resour. Res.*, vol. 53, no. 1, pp. 283–301, Jan. 2017.
[28] P. J. Starks, G. C. Heathman, T. J. Jackson, and M. H. Cosh, "Temporal stability of soil moisture profile," *J. Hydrol.*, vol. 324, no. 1–4, pp. 400–411, 2006.
[29] L. Zhao et al., "Spatiotemporal analysis of soil moisture observations within a Tibetan mesoscale area and its implication to regional soil moisture measurements," *J. Hydrol.*, vol. 482, pp. 92–104, 2013.
[30] J. Dari, R. Morbidelli, C. Saltalippi, C. Massari, and L. Brocca, "Spatial-temporal variability of soil moisture: Addressing the monitoring at the catchment scale," *J. Hydrol.*, vol. 570, pp. 436–444, Mar. 2019.

[31] K. Schneider, J. Huisman, L. Breuer, Y. Zhao, and H.-G. Frede, "Temporal stability of soil moisture in various semi-arid steppe ecosystems and its application in remote sensing," *J. Hydrol.*, vol. 359, no. 1/2, pp. 16–29, 2008.
[32] M. S. Yee, J. P. Walker, A. Monerris, C. Rüdiger, and T. J. Jackson, "On the identification of representative in situ soil moisture monitoring stations for the validation of SMAP soil moisture products in Australia," *J. Hydrol.*, vol. 537, pp. 367–381, 2016.
[33] H. A. Bhatti, T. Rientjes, W. Verhoef, and M. Yaseen, "Assessing temporal stability for coarse scale satellite moisture validation in the Maqu area, Tibet," *Sensors (Basel)*, vol. 13, no. 8, pp. 10725–10748, Aug. 2013.
[34] L. Zhang, C. He, and M. Zhang, "Multi-scale evaluation of the SMAP product using sparse In-situ network over a high mountainous watershed, Northwest China," *Remote Sens.*, vol. 9, no. 11, 2017, Art. no. 1111.
[35] T. Zhao et al., "Soil moisture experiment in the Luan River supporting new satellite mission opportunities," *Remote Sens. Environ.*, vol. 240, 2020, Art. no. 111680.
[36] A. Colliander et al., "Validation of soil moisture data products from the NASA SMAP mission," *IEEE J. Sel. Topics Appl. Earth Observ. Remote Sens.*, vol. 15, pp. 364–392, 2022.
[37] A. Tavakol, V. Rahmani, S. M. Quiring, and S. V. Kumar, "Evaluation analysis of NASA SMAP L3 and L4 and SPoRT-LIS soil moisture data in the United States," *Remote Sens. Environ.*, vol. 229, pp. 234–246, 2019.
[38] E. Jalilvand, R. Abolafia-Rosenzweig, M. Tajrishy, and N. N. Das, "Evaluation of SMAP/Sentinel 1 high-resolution soil moisture data to detect irrigation over agricultural domain," *IEEE J. Sel. Topics Appl. Earth Observ. Remote Sens.*, vol. 14, pp. 10733–10747, 2021.
[39] F. Mohseni, S. M. Mirmazloumi, M. Mokhtarzade, S. Jamali, and S. Homayouni, "Global evaluation of SMAP/Sentinel-1 soil moisture products," *Remote Sens.*, vol. 14, no. 18, Sep. 2022, Art. no. 4624.
[40] A. Colliander et al., "Validation of SMAP surface soil moisture products with core validation sites," *Remote Sens. Environ.*, vol. 191, pp. 215–231, 2017.
[41] P. Lal, G. Singh, N. N. Das, A. Colliander, and D. Entekhabi, "Assessment of ERA5-land volumetric soil water layer product using in situ and SMAP soil moisture observations," *IEEE Geosci. Remote Sens. Lett.*, vol. 19, 2022, Art. no. 2508305.
[42] J. S. Famiglietti, D. Ryu, A. A. Berg, M. Rodell, and T. J. Jackson, "Field observations of soil moisture variability across scales," *Water Resour. Res.*, vol. 44, no. 1, pp. 1–16, 2008.
[43] J. M. Jacobs, B. P. Mohanty, E. C. Hsu, and D. Miller, "SMEX02: Field scale variability, time stability and similarity of soil moisture," *Remote Sens. Environ.*, vol. 92, no. 4, pp. 436–446, Sep. 2004.
[44] L. Gao, Y. Wang, J. Geris, P. D. Hallett, and X. Peng, "The role of sampling strategy on apparent temporal stability of soil moisture under subtropical hydroclimatic conditions," *J. Hydrol. Hydromechanics*, vol. 67, no. 3, pp. 260–270, 2019.
[45] X. Gao et al., "Estimation of spatial soil moisture averages in a large gully of the Loess Plateau of China through statistical and modeling solutions," *J. Hydrol.*, vol. 486, pp. 466–478, 2013.
[46] J. Zeng, P. Shi, K.-S. Chen, H. Ma, H. Bi, and C. Cui, "Assessment and error analysis of satellite soil moisture products over the third pole," *IEEE Trans. Geosci. Remote Sens.*, vol. 60, pp. 1–18, 2022.
[47] A. Gruber et al., "Validation practices for satellite soil moisture retrievals: What are (the) errors?," *Remote Sens. Environ.*, vol. 244, 2020, Art. no. 111806.
[48] H. Vereecken, T. Kamai, T. Harter, R. Kasteel, J. Hopmans, and J. Vanderborght, "Explaining soil moisture variability as a function of mean soil moisture: A stochastic unsaturated flow perspective," *Geophysical Res. Lett.*, vol. 34, no. 22, pp. 1–6, 2007.
[49] L. Brocca, T. Tullo, F. Melone, T. Moramarco, and R. Morbidelli, "Catchment scale soil moisture spatial–temporal variability," *J. Hydrol.*, vol. 422–423, pp. 63–75, 2012.

Longfei Hao received the B.S. degree in surveying and mapping engineering in 2022 from the School of Surveying and Land Information Engineering, Henan Polytechnic University, Jiaozuo, China, where he is currently working toward the M.S. degree in surveying and mapping engineering.

His research interest includes microwave remote sensing of soil moisture.

Jingjing Chen received the B.S. degree in civil engineering from the School of Civil Engineering, Henan Polytechnic University, Jiaozuo, China, in 2012.

She is currently an Assistant Professor with the Xinyang Vocational and Technical College, Henan, China. Her research interests include remote sensing and machine learning.

Zushuai Wei received the Ph.D. degree in photogrammetry and remote sensing from Wuhan University, Wuhan, China, in 2019.

Currently, he is an Assistant Professor with Jianghan University, Wuhan, China. His research interests include microwave remote sensing of soil moisture and its downscaling.

Linguang Miao received the B.S. degree in surveying and mapping engineering from the School of Surveying and Urban Spatial Information, Henan University of Urban Construction, Henan, China, in 2021. He is currently working toward the M.S. degree in photogrammetry and remote sensing from the School of Surveying and Land Information Engineering, Henan Polytechnic University, Jiaozuo, China.

His research interests include hydrological remote sensing and machine learning.

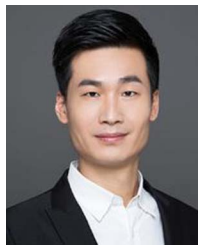

Tianjie Zhao (Senior Member, IEEE) received the B.S. and Ph.D. degrees in cartography and geographical information system from Beijing Normal University, Beijing, China, in 2007 and 2012, respectively.

From 2010 to 2012, he was a Visiting Scientist with the Hydrology and Remote Sensing Laboratory, Agricultural Research Service (ARS), U.S. Department of Agriculture, Beltsville, MD, USA. Currently, he is a Research Professor with the State Key Laboratory of Remote Sensing Science, Aerospace Information Research Institute, Chinese Academy of Sciences (CAS), Beijing, China. His research interests include microwave remote sensing of soil moisture and its freeze-thaw process.

Dr. Zhao was the recipient of the scholarship award for excellent doctoral student granted by the Ministry of Education of China in 2011, the Young Scientist Award from the International Union of Radio Science (URSI) in 2014, and the Young Scientist Award from Progress in Electromagnetics Research Symposium (PIERS) in 2018.

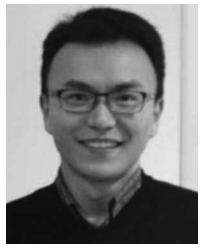

Jian Peng received the Ph.D. degree in Earth sciences from the Max Planck Institute for Meteorology, University of Hamburg, Hamburg, Germany, in 2013.

He is currently the Head of the Department of Remote Sensing with the UFZ, Leipzig, Germany, and a Full Professor for Hydrology and Remote Sensing with the University of Leipzig, Leipzig, Germany. His research interests include quantitative retrieval of land surface parameters from Earth observations, with a special emphasis on evapotranspiration and soil moisture, and the development of downscaling schemes, as well as the application of remote sensing products in hydrological and meteorological studies.